Parametric study of FRP-strengthened reinforced concrete panels under blast

loads

†X. Lin¹ and *Y.X. Zhang²

¹School of Civil and Environmental Engineering, Nanyang Technological University, Singapore.

²School of Engineering and Information Technology, the University of New South Wales, Australian Defence Force Academy, Australia

*Presenting author: y.zhang@adfa.edu.au †Corresponding author: xslin@ntu.edu.sg

Abstract

The use of fibre reinforced polymer (FRP) as a strengthening material for reinforced concrete structures to resist blast loads has attracted great interests in recently years. The structural responses of FRP-strengthened reinforced concrete panels under blast loads are investigated intensively in this paper by employing a finite element model recently developed by the authors. The effects of the thickness of the strengthening FRP sheet, the retrofitted surface, the standoff distance and the mass of the charge on the structural behavior of the reinforced concrete panels under blast loads are studied. The results of the parametric study are analyzed and presented in this paper.

Keywords: FRP, Reinforced concrete panel, Blast loading, Finite element model

Introduction

In recent years, fibre reinforced polymers (FRPs) have been increasingly used for retrofitting reinforced concrete (RC) structural components to against blast accidents which could produce an overload pressure much greater than the design load of a structure in a very short period of time and result in severe damage to the RC structure. The FRP attachments can significantly improve the blast resistance of structures without forfeiting usable space [Nam et al. (2010)]. FRP is also considered to be one of the most suitable materials for retrofitting concrete structures under blast loads, as it can be easily installed and naturally blended to the structures [Nam et al. (2009)].

A few experimental studies on the FRP-strengthened RC panels subjected to blast loads have been reported. However, full scale experimental tests are usually costly and time consuming. By contrast, finite element analysis is a much more economical and efficient method for predicting the behaviors of RC structures and structural components especially for the investigation of the parametric effects. Several numerical studies for the analysis of FRP-strengthened RC panels under blast loads [Nam et al. (2010); Nam et al. (2009); Mosalam and Mosallam (2001)] were conducted. However, the finite element models employed in these researches were either not very well validated or didn't consider the strain rate effect on the material properties of FRP appropriately. A finite element model, which considered the strain rate effect on FRP materials, was established by Tanapornraweekit et al. [Tanapornraweekit et al. (2010)] for modelling the structural behavior of GFRP and CFRPstrengthened reinforced concrete slabs under air blasts. Although progress has been made in the numerical modelling of FRP-strengthened RC structures under blast loading, the numerical models developed are still far from ideal due to the complexity of dynamic response of reinforced concrete structures and the lack of information on the dynamic material properties of FRPs. Moreover, a comprehensive study on the structural responses of FRP-strengthened RC panels under blast loads affected by various parameters has rarely been reported.

Recently, a 3D finite element model was developed by the authors for the analysis of the structural behavior of FRP strengthened RC panels under blast loading [Lin et al. (2015)]. In this model, strain rate effects on the material models of concrete under tension and compression were considered separately, and strain rate effects on the material models of steel reinforcements and FRP laminates were also taken into account. The proposed finite element model was demonstrated to be effective and accurate for the prediction of the structural behavior of FRP-strengthened RC panels under blast loads. In this paper, the 3D finite element model is firstly introduced, and then it is employed to investigate the effects of a series of parameters on the structural behaviors of FRPstrengthened RC panels under blast loads, including the effects of the thickness of FRP sheet, the retrofitted surface, the standoff distance and the mass of the charge. The research findings are reported in this paper, which are expected to be able to provide reliable and useful references for structural design.

A 3D Finite Element Model

The 3D nonlinear finite element model was established using the commercial software package LS-DYNA. Concrete was modelled using the Solid 164 element, which is an 8-node constant stress hexahedron brick element, and the Lagrangian formulation was applied in the analysis. Steel reinforcing bars were modelled using the Link 160 truss element, and FRP laminates were modelled using the Shell 163 element, which is a 4-noded element with both bending and membrane capabilities. A perfect bond was assumed both between concrete and steel reinforcements and between FRP laminates and concrete panel.

Material Model for Concrete

The MAT72 R3 was employed for modelling the concrete. In the study conducted by Lin et al. [Lin et al. (2014)], various material models available for the analysis of concrete structures under dynamic loading were compared, and that the CONCRETE DAMAGE REL3 (MAT72 R3) in LS-DYNA was found to be relatively simple and numerically robust. It can reproduce the key concrete behaviors which are critical to blast and impact analyses, and it is also easy to be calibrated using laboratory data [Magallanes et al. (2010)].

In addition, concrete dynamic behavior is strain rate dependent. Both tensile and compressive strengths of concrete can be increased significantly under dynamic loading. In MAT72 R3, the strain rate effect is accounted for by using a dynamic increase factor (DIF), which is the ratio of the dynamic-to-static material strength. In the developed finite element model, the values of DIF suggested by CEB-FIP Model Code 1990 [CEB-FIP (1993)] were employed for concrete in compression, while the modified formulations proposed by Malvar and Crawford [Malvar and Crawford (1998)] were used for concrete in tension. The formulas of DIF for concrete in compression and tension are given in the following equations.

For concrete in compression:
$$\text{CDIF} = \frac{f_{c,d}}{f_{c,s}} = \left(\frac{\dot{\varepsilon}_c}{\dot{\varepsilon}_{co}}\right)^{1.026\alpha} \qquad \text{for} \qquad \dot{\varepsilon}_c \leq 30 \, \text{s}^{-1} \qquad (1a)$$

$$\text{CDIF} = \frac{f_{c,d}}{f_{c,s}} = \gamma \left(\frac{\dot{\varepsilon}_c}{\dot{\varepsilon}_{co}}\right)^{1/3} \qquad \text{for} \qquad \dot{\varepsilon}_c > 30 \, \text{s}^{-1} \qquad (1b)$$

$$CDIF = \frac{f_{c,d}}{f_{c,c}} = \gamma \left(\frac{\dot{\varepsilon}_c}{\dot{\varepsilon}_{c,c}}\right)^{1/3} \qquad \text{for} \qquad \dot{\varepsilon}_c > 30 \,\text{s}^{-1}$$
 (1b)

where $f_{c,d}$ is the dynamic compressive strength of concrete, $f_{c,s}$ the static compressive strength of concrete, $\dot{\varepsilon}_c$ the strain rate in compression, and $\dot{\varepsilon}_{co} = 30 \times 10^{-6} \, \text{s}^{-1}$ the quasi-static strain rate in compression. α is the coefficient given by $\alpha = 1/(5 + 9f_{c,s}/10)$, and γ is expressed as $\log \gamma = 6.156\alpha - 2$

For concrete in tension:

$$TDIF = \frac{f_{ct,d}}{f_{ct,s}} = \left(\frac{\dot{\varepsilon}_{ct}}{\dot{\varepsilon}_{cto}}\right)^{\delta} \qquad \text{for} \qquad \dot{\varepsilon}_{ct} \le 1 \,\text{s}^{-1}$$
 (2a)

$$TDIF = \frac{f_{ct,d}}{f_{ct,s}} = \beta \left(\frac{\dot{\varepsilon}_{ct}}{\dot{\varepsilon}_{cto}}\right)^{1/3} \qquad \text{for} \qquad \dot{\varepsilon}_c > 1 \, s^{-1}$$
 (2b)

where $f_{\text{ct,d}}$ is the dynamic tensile strength of concrete, $f_{\text{ct,s}}$ the static tensile strength of concrete, $\dot{\varepsilon}_{\text{ct}}$ the strain rate in tension, and $\dot{\varepsilon}_{\text{cto}} = 1 \times 10^{-6} \text{ s}^{-1}$ the quasi-static strain rate in tension. δ is the coefficient given by $\delta = 1/(1 + 8f_{c,s}/10)$, and β is expressed as $\log \beta = 6\delta - 2$.

Due to the presence of strain-softening phenomenon in concrete, non-converged or incorrect converged solutions are usually obtained from finite element analysis, and the results are not objective with regard to mesh refinement [de Borst (1987)]. Therefore, a localization limiter must be introduced in concrete material model to remedy this situation. In the MAT72 R3, a crack band model is employed for this spurious mesh sensitivity caused by the strain-softening. In the single element tests carried out by Lin et al. [Lin et al. (2014)], the softening of small elements was found to be relatively slow. With the increase in element size, the softening was accelerated to maintain constant fracture energy. The stress-strain relationships for the elements with size between 1 mm and 25 mm were found to coincide very well. Therefore, the size of finite element mesh in the present model was chosen to be 15 mm.

Material Model for Steel

In the proposed finite element model, steel reinforcing bars were modelled using the PLASTIC KINEMATIC Model (MAT3). The isotropic and kinematic hardening can be specified by varying the hardening parameter between 0 and 1. The Cowper-Symonds model [Hallquist (2006)] was used to take into account the strain rate effect under blast loading, which scaled the yield stress by a strain-rate dependent factor of $1 + (\dot{\varepsilon}/C)^{1/P}$, where $\dot{\varepsilon}$ is the strain rate, and C and P are the strain rate parameters for Cowper-Symonds model, which were 255.4 and 7.59 respectively in the proposed model.

Material Model for FRPs

The material properties of FRPs are also strain rate sensitive, and their modulus and strength increase with the increasing of the loading rate. So far, very few constitutive relationships of FRPs considering dynamic loading effect have been reported in the literature, and the use of an improper material model for FRPs under high strain rate might lead to inaccuracy in modelling the structural performance of FRP-strengthened RC structures subjected to blast loading. In the proposed finite element model, FRP laminates were modelled using the PLASTICITY_POLYMER Model (MAT89), and the strain rate effect on FRP material properties were taken into account by employing the formulas used by Tanapornraweekit et al. [Tanapornraweekit et al. (2010)] for glass fibre reinforced polymer (GFRP) and carbon fibre reinforced polymer (CFRP) laminates. The formulas for GFRP laminates are given as follows.

Elastic modulus of GFRP (unit: GPa):

$$E_{d} = E_{s}$$
 for $\dot{s} < 0.01 \, s^{-1}$ (3a)

$$E_d = E_s + 13.969 \log \dot{\varepsilon} - 27.606$$
 for $200 \, s^{-1} < \dot{\varepsilon} \le 1700 \, s^{-1}$ (3c)

Tensile strength of GFRP (unit: GPa):

$$f_d = f_s$$
 for $\dot{\varepsilon} < 0.01 \, s^{-1}$ (4a)
 $f_d = f_s + 0.2797 \log \dot{\varepsilon} + 0.5594$ for $0.01 \, s^{-1} \le \dot{\varepsilon} \le 90 \, s^{-1}$ (4b)
 $f_d = f_s + 0.6696 \log \dot{\varepsilon} - 0.2026$ for $90 \, s^{-1} < \dot{\varepsilon} \le 1700 \, s^{-1}$ (4c)

Failure strain of GFRP:

$$\varepsilon_d = \varepsilon_s$$
 for $\dot{\varepsilon} < 0.01 \, s^{-1}$ (5a)
 $\varepsilon_d = \varepsilon_s + 0.005 \log \dot{\varepsilon} + 0.01$ for $0.01 \, s^{-1} \le \dot{\varepsilon} \le 1700 \, s^{-1}$ (5b)

where E_{d} , f_{d} and E_{d} are the dynamic elastic modulus, tensile strength and failure strain of GFRP respectively, E_{s} , f_{s} and E_{s} the static elastic modulus, tensile strength and failure strain of GFRP respectively, and E_{s} is the strain rate.

Numerical Analysis

The developed finite element model has been validated by the authors [Lin et al. (2015)] by modelling two RC concrete panels strengthened with GFRP laminates. The two reinforced concrete panels (Panel b was the repeat test specimen of Panel a) had the same design and were supported on two short edges by a steel frame. They were reinforced on both top and bottom with 6 mm longitudinal steel bars spaced at 225 mm centre to centre, and 6 mm transverse steel bars at 300 mm centre to centre. In addition, 6 mm steel reinforcing bars were placed on both sides of the support zone at 65 mm centre to centre space. The yield strength, ultimate strength, ultimate strain and elastic modulus of steel reinforcing bars were 356 MPa, 412 MPa, 22.2% and 194 GPa, respectively. The compressive strength of concrete was 32 MPa. A 0.353 mm thick single layer GFRP sheet was attached to the top and bottom faces of the reinforced concrete panels. The Young's modulus and tensile strength of the GFRP were 75.6 GPa and 1331 MPa, respectively. The GFRP-strengthened RC panels were subjected to a blast load caused by a charge with an equivalent TNT mass of 0.45 kg, which was placed at 0.5 m above the centre of the concrete panel. The central displacementtime histories obtained from the developed finite element model, the tests and Tanapornraweekit et al.'s numerical analysis [Tanapornraweekit et al. (2010); Tanapornraweekit et al. (2011)] are shown in Fig. 1.

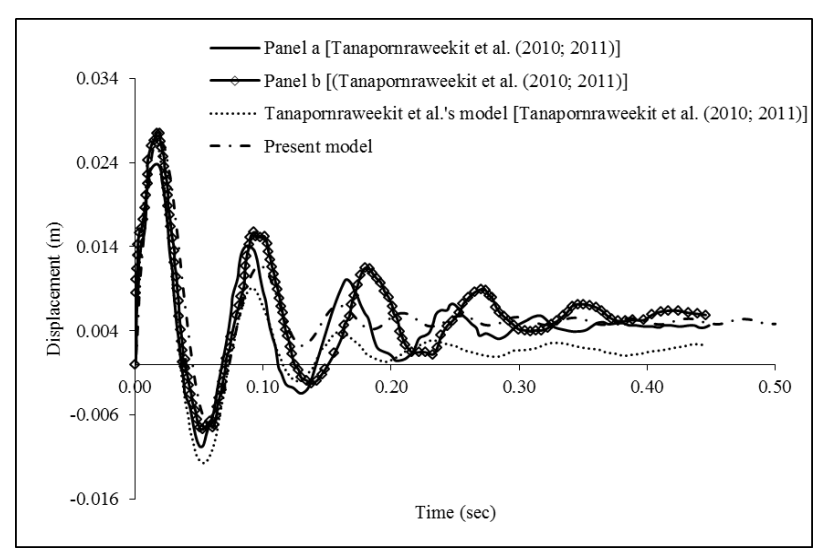


Figure 1. Central displacement-time histories of Panel a and Panel b

It can be seen that the computed results agree very well with the test data, and they are closer to the test results than Tanapornraweekit et al.'s prediction [Tanapornraweekit et al. (2010)], especially

for the residual deflection. The maximum and residual deflections of the GFRP-strengthened reinforced concrete panel obtained from the present model are 27.2 mm and 5.3 mm respectively.

In this study, the developed finite element model is employed to further investigate the structural responses of FRP-strengthened RC panels affected by various parameters, including the effects of the thickness of the FRP sheet, the retrofitted surface, the standoff distance and the mass of the charge. The GFRP-strengthened RC panels (Panel a and Panel b) are used herein as a basic model, and the material properties of concrete, steel and GFRP sheet retain the same. In the parametric study, the TNT charge mass varies from 0.30 kg to 0.75 kg, and the standoff distance from 0.3 m to 1.0 m. In the basic model, the RC panel is strengthened by the GFRP sheets of the same thickness on both top and bottom surfaces of the panel. In order to investigate the FRP strengthening effect, the thickness of the FRP sheets on the top and bottom surfaces are changing from 0 to 1.0 mm and from 0.353 mm to 1.0 mm respectively, thus the modelled RC panels either have thicker GFRP sheet strengthened on the bottom surface or have GFRP sheet of the same thickness on both top and bottom surfaces. The details of various parameters and the predicted maximum and residual deflections of the concrete panels are listed in Tabel 1. Figs. 2 to 4 show the central displacement-time histories of GFRP-strengthened RC panels with various parameters.

As can be seen, with the increase of TNT charge mass, both the maximum and residual deflections of the GFRP-strengthened RC panels increase significantly. The maximum deflection of the panel under the blast of a charge mass of 0.30 kg TNT is 53.3%, 35.4% and 15.1% of that of the 0.45 kg, 0.60 kg and 0.75 kg TNT respectively. The residual deflection of the panel subjected to 0.30 kg TNT is 2.2 mm, which is 41.5%, 31.9% and 13.7% of that under 0.45 kg, 0.60 kg and 0.75 kg TNT blast loads respectively. For the same TNT charge mass, the maximum and residual deflections of GFRP-strengthened RC panels decrease with the increase of the standoff distance. The maximum and residual deflections for the panel with a standoff distance of 1.0 m are 9.5 mm and 2.7 mm respectively, which are only 34.9% and 50.9% respectively of those obtained for the panel with a standoff distance of 0.5 m. Both the maximum and residual deflections increase when the standoff distance reduces from 0.5 m to 0.4 m, but not by much. Whereas, when the standoff distance is further reduced from 0.4 m to 0.3 m, the maximum and residual deflections of panel suddenly jump to 126.8 mm and 48.5 mm respectively, which are about 4 times and 10 times of those for the panel at 0.4 m away from the charge.

In addition, the thickness of the FRP strengthening sheet also affects the blast resistance of RC panels. In general, the maximum and residual deflections of the RC panels are reduced with the increase of the thicknesses of the FRP strengthening sheets. The maximum deflection of the RC panel with 1.0 mm GFRP sheets strengthened on both surfaces is 19.7 mm, which is 72.4% of that for the basic model with 0.353 mm GFRP sheet. The residual deflection is reduced from 5.3 mm to 1.8 mm which is only 34.0% of the deflection in the basic model. Also, the RC panels strengthened with GFRP sheets of different thicknesses on the top and bottom surfaces are modelled in this study. By comparing the basic model with the panel without GFRP sheet strengthened on the top surface, it is found that the maximum deflection of the basic model is reduced by 4.2%, whereas the residual deflection is increased from 0 to 5.3 mm. When the thickness of the GFRP sheet on the top surface is kept constant as 0.353 mm, and that on the bottom surface is increased, the computed maximum and residual deflections are always a bit less than those obtained for the panel which has the same GFRP thickness on the top and bottom surfaces. However, it should be noted that the deflection when the panel bounces back is obviously reduced by strengthening the GFRP sheets with the same thicknesses on both surfaces, as can be seen in Fig. 4. Therefore, the damage on the top surface of the RC panels could be reduced by increasing the thickness of GFRP sheets on the top surface.

Table 1. Maximum and residual deflections affected by various parameters

TNT Charge mass (kg)	Standoff distance (m)	GFRP thickness (mm)		Maximum	Residual
		Bottom (B)	Top (T)	deflection (mm)	deflection (mm)
0.30	0.5	0.353	0.353	14.5	2.2
0.45	0.5	0.353	0.353	27.2	5.3
0.60	0.5	0.353	0.353	41.0	6.9
0.75	0.5	0.353	0.353	96.3	16.1
0.45	0.3	0.353	0.353	126.8	48.5
0.45	0.4	0.353	0.353	33.6	5.0
0.45	0.5	0.353	0.353	27.2	5.3
0.45	0.75	0.353	0.353	16.8	3.4
0.45	1.0	0.353	0.353	9.5	2.7
0.45	0.5	0.353	0	28.4	0
0.45	0.5	0.353	0.353	27.2	5.3
0.45	0.5	0.5	0.353	23.0	1.8
0.45	0.5	0.5	0.5	25.8	4.3
0.45	0.5	1.0	0.353	18.4	-0.7
0.45	0.5	1.0	1.0	19.7	1.8

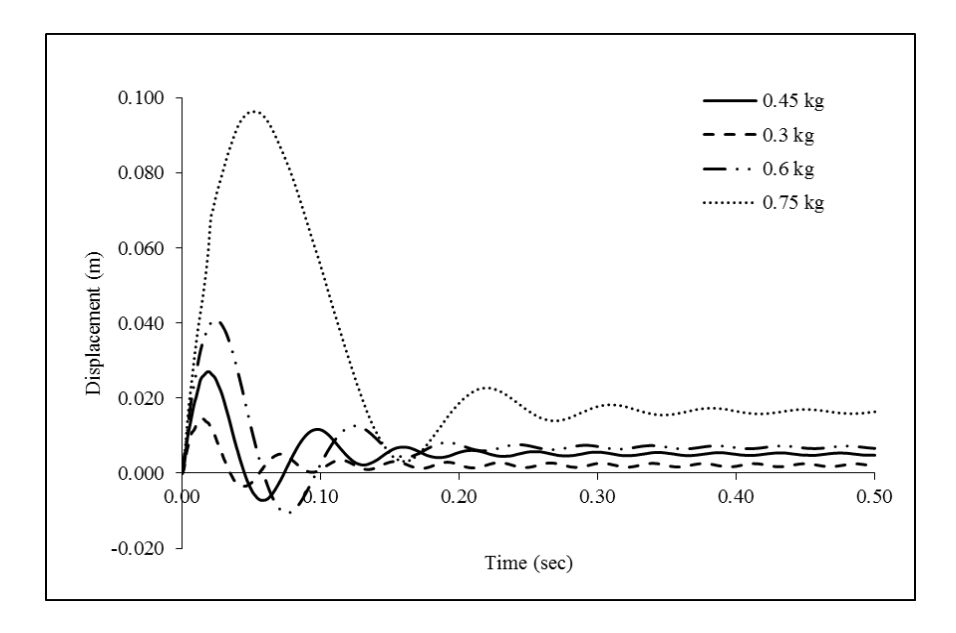


Figure 2. Displacement-time histories of GFRP-strengthened RC panels under various TNT charge masses

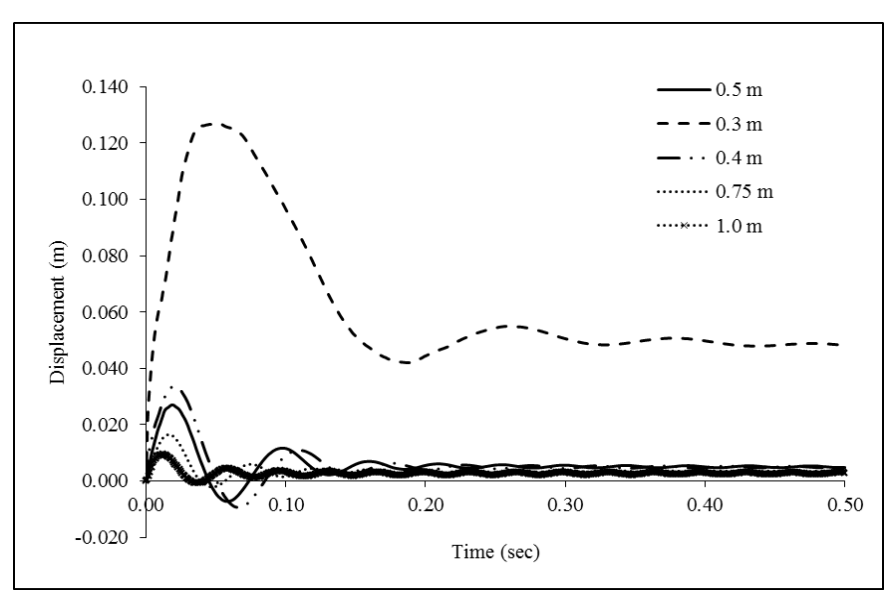


Figure 3. Displacement-time histories of GFRP-strengthened RC panels at various standoff distances

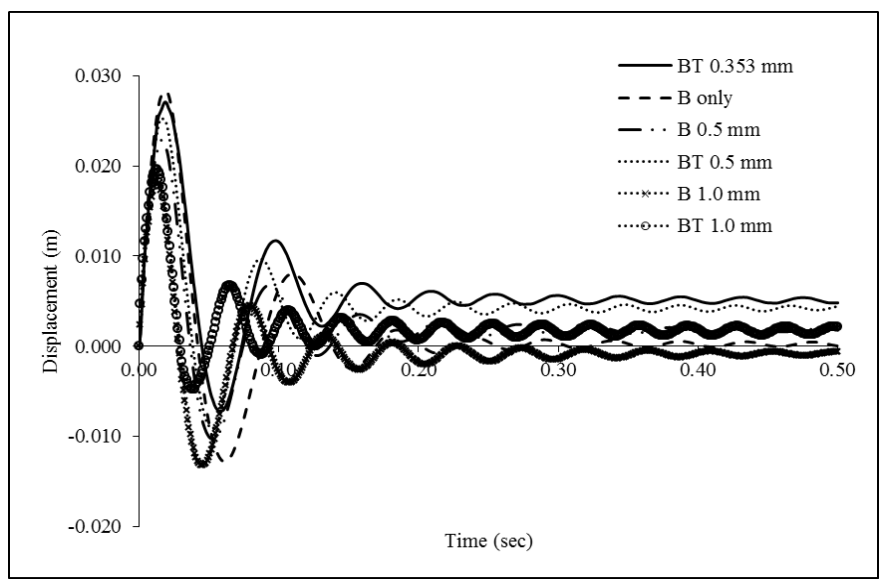


Figure 4. Displacement-time histories of RC panels with various strengthening laminates under blast loads

Conclusions

In this paper, a finite element model recently developed for modelling structural behavior of FRP-strengthened RC panels under blast loads is firstly introduced, and then employed to investigate the responses of FRP-strengthened RC panels with various parameters under blast loads. It is found that the structural behavior of FRP-strengthened RC panel is very sensitive to the charge mass and the standoff distance. Care must be taken in the structural design, especially when increasing the charge mass or reducing the standoff distance. In addition, the effect of thickness of GFRP sheet on different retrofitting surface is studied. In general, with the increase in the thickness of the GFRP sheet, both the maximum and residual deflections of RC panel are decreased. Although no improvement in reducing the maximum and residual deflections could be observed by using thicker GFRP sheet on the top surface, the deflection when the RC panel bounces back could be reduced greatly.

References

- Nam, J.-W., Kim, H.-J., Kim, S.-B., Yi, N.-H. and Kim, J.-H. J. (2010) Numerical evaluation of the retrofit effectiveness for GFRP retrofitted concrete slab subjected to blast pressure, *Composite Structures* **92**, 1212-1222.
- Nam, J.-W., Kim, H.-J., Kim, S.-B., Kim, J.-H. J. and Byun, K. J. (2009) Analytical study of finite element models for FRP retrofitted concrete structure under blast loads, *International Journal of Damage Mechanics* **18**, 461-490.
- Mosalam, K. M. and Mosallam, A. S. (2001) Nonlinear transient analysis of reinforced concrete slabs subjected to blast loading and retrofitted with CFRP composites, *Composites Part B: Engineering* **32**, 623-636.
- Tanapornraweekit, G., Haritos, N., Mendis, P. and Ngo, T. (2010) Finite element simulation of FRP strengthened reinforced concrete slabs under two independent air blasts, *International Journal of Protective Structures* 1, 469-488.
- Lin, X., Zhang, Y. X. and Lee, C. K. (2015) Finite element analysis of FRP-strengthened reinforced concrete panels under blast loading, 5th International Conference on Design and Analysis of Protective Structures, 19-21 May 2015, Singapore (submitted).
- Lin, X., Zhang, Y. X. and Hazell, P. J. (2014) Modelling the response of reinforced concrete panels under blast loading, *Materials & Design* **56**, 620-628.
- Magallanes, J. M., Wu, Y., Malvar, L. J. and Crawford, J. E. (2010) Recent improvements to Release III of the K&C concrete model, 11th International LS-DYNA Users Conference.
- Comite Euro-International du Beton (1993) CEB-FIP model code 1990, Lausanne: Thomas Telford Services Ltd.
- Malvar, L. J. and Crawford, J. E. (1998) Dynamic increase factors for concrete, Naval Facilities Engineering Service Center, Port Hueneme, CA.
- de Borst, R. (1987) Computation of post-bifurcation and post-failure behavior of strain-softening solids, *Computers & Structures* **25**, 211-224.
- Hallquist, J. O. (2006) *LS-DYNA theory manual*, Livermore Software Technology Corporation (LSTC), Livermore, CA. Tanapornraweekit, G., Haritos, N. and Mendis, P. (2011) Behavior of FRP-RC slabs under multiple independent air blasts, *Journal of Performance of Constructed Facilities* **25**, 433-440.